

Molecular dynamics simulations of motion of edge and screw dislocations in a metal

Jinpeng Chang ^{a,*}, Wei Cai ^a, Vasily V. Bulatov ^b, Sidney Yip ^a

^a *Department of Nuclear Engineering, Massachusetts Institute of Technology, Cambridge, MA 02139, USA*

^b *Lawrence Livermore National Laboratory, University of California, Livermore, CA 94550, USA*

Accepted 1 June 2001

Abstract

Motions of a straight edge dislocation and a kinked screw dislocation in BCC Mo, described by the Finnis–Sinclair potential, are studied in periodic simulation cells subjected to an applied shear stress. Procedures for setting up the initial atomic configurations in each case are described, and estimate is made of the local driving force due to the image interactions. Preliminary results show that at low temperature the edge dislocation moves primarily through kink nucleation, whereas the mobility of the screw dislocation is strongly facilitated by the presence of a kink. © 2002 Elsevier Science B.V. All rights reserved.

Keywords: Dislocation mobility; Molecular dynamics; Periodic image effect

1. Introduction

Molecular dynamics (MD) simulation is a powerful method for probing the structure and dynamics of extended crystalline defects like grain boundaries [1] and dislocations [2,3]. While the velocity of an isolated dislocation in an fcc metal has been obtained using fixed border conditions to transmit the driving force [4,5], very little is known about the underlying mechanistic details, such as the role of kinks on the mobility of a straight dislocation. Another issue that has not been addressed adequately is how a specific border con-

dition modifies the local driving force acting on the defect core.

In this brief report we discuss an attempt to simulate by MD the motions of two types of dislocations in a bcc metallic lattice, an initially straight edge dislocation and a screw dislocation with a pre-existing kink. We focus first on the methodological issue of setting up the appropriate atomic configurations in a periodic simulation cell. The decision to adopt the periodic boundary conditions (PBC) stems mainly from the fact that the image interaction effects associated with PBC have recently been clarified [6], to the extent that one now knows how to estimate self-consistently the magnitude of these effects, as we will discuss briefly here. We then present preliminary MD results for Mo, obtained using the Finnis–Sinclair empirical

* Corresponding author.

E-mail address: jpchang@mit.edu (J. Chang).

potential model [7] as revised by Ackland and Thetford [8], which suggest quite different roles for kink defects in the mobility of edge and screw dislocations at low temperature. An edge dislocation appears to move primarily by kink nucleation, with kink migration being relatively unimportant; in contrast, the mobility of a screw dislocation is greatly enhanced by the presence of a kink.

2. Dislocation dipole setup

In an atomistic simulation cell with PBC, the topological constraint of vanishing total Burgers vector means that dislocations have to be introduced at least in pair, in the form of a dipole. Fig. 1 shows the specific procedure we are adopting to create a particular edge dislocation dipole. Starting with a rectangular atomic cell with box vectors at $6[111]$, $24[\bar{1}01]$ and $36[1\bar{2}1]$, respectively, we first remove a layer of atoms on an (111) plane (the shaded region) and then displace all other atoms according to the linear elastic displacement field of a dislocation dipole in a periodic cell [9]. After conjugate gradient relaxation, we obtain an atomic configuration with two edge dislocations with opposing Burgers vector $1/2[111]$, each lying on a $(\bar{1}01)$ glide plane and separated from the other by a distance of $12[\bar{1}01]$. The inset in Fig. 1 shows the detailed relaxed atomic arrangement around the dislocation core. In this set up of the initial con-

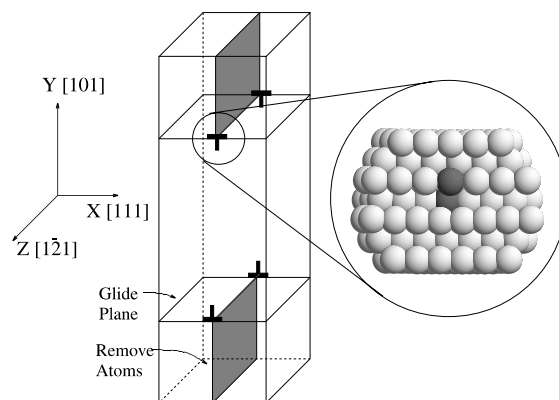


Fig. 1. Setting up an edge dislocation dipole by removing a layer of atoms in the shaded plane, followed by conjugate gradient force relaxation. Atomic arrangement around the dislocation core is shown with the core atoms (highlighted) having the largest potential energy as well as maximum disregistry across the two atomic layers on the either side of the glide plane.

figuration in a periodic simulation cell, the two dislocations can move in opposite directions naturally without annihilating each other because of the absence of vacancies (none introduced and low temperature).

In contrast to edge dislocation dipoles, screw dislocation dipoles cannot be created by removing atoms. As shown in Fig. 2(a), taking a cell with box vectors $4[11\bar{2}]$, $14[1\bar{1}0]$ and $5[111]$, we make a cut on the $(11\bar{2})$ plane and displace the two ad-

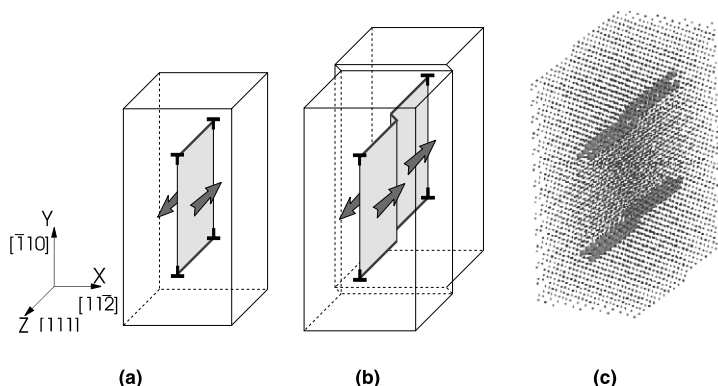


Fig. 2. (a) Creation of screw dislocation dipole in a PBC simulation cell by displacing the two layers of atoms besides the cut plane by b relative to each other, followed by force relaxation. (b) Creation of kinks on screw dislocation by putting two copies of cells in (a) with an $1/2[11\bar{1}]$ in between. (c) Atomic arrangement of (b).

adjacent layers of atoms by $b = 1/2[111]$ relative to each other. The remaining atoms are again displaced according to the linear elastic displacement field of the dislocation dipole, and the atomic arrangement relaxed using conjugate gradient. Because straight screw dislocations move much slower than edge dislocations, and if they do move (at either high temperature or high stresses) they can annihilate with each other via cross slip, we will at the outset introduce a single kink into the initially straight screw dislocations, with the expectation that the pre-existing kink will significantly enhance the dislocation mobility. Moreover, since the kink is effectively a short dislocation with edge character, it will have the effect of confining the screw dislocation to its glide plane. As shown in Fig. 2(b), we create kinks on the two screw dislocations by placing two copies of the cell in Fig. 2(a) with an $1/2[111]$ offset between them. The basis vector along the dislocation line is redefined; it is no longer parallel to $[111]$, so that the kink leaving the cell at one end re-enters the cell from the other end [10]. The configuration is then relaxed by conjugate gradient method yielding the atomic arrangements in Fig. 2(c), where three columns of atoms at the dislocation cores are plotted in larger spheres than background atoms. This particular system contains 6845 atoms.

3. Image effects in a periodic simulation cell

The problem of dislocation motion generally refers to the movement of a single dislocation moving in an infinite lattice. To relate this problem to that of a dislocation dipole, two effects need to be considered, one is the interaction between the two dislocation forming the dipole and the other is the interaction between these two dislocations and their images which are introduced by the PBC. Both interactions may be treated in the framework of linear elasticity. We will denote the interaction energy associated with these two effects as E_{elas} ; it is actually an energy per unit length of dislocation. Recently a method for calculating E_{elas} has been obtained [6]. We will apply this result to give an estimate of local driving force acting on the dislocation.

From linear elasticity and atomistic simulations we find that E_{elas} varies in an oscillatory manner with the offset x (along X direction in Fig. 1) between the two dislocations forming the dipole. We can define the maximum slope $\max dE_{\text{elas}}/dx = \sigma_{\text{int}}b$ as a measure of the total effect of PBC, where σ_{int} is the maximum internal stress acting on the dislocation with b the Burgers vector. For the simulation cell shown in Fig. 1, the variation of E_{elas} can be well represented by a sinusoidal function, $E_{\text{elas}} = A \sin(x/12b) + \text{const.}$, where $A = 0.98 \times 10^{-3} \text{ eV/\AA}$. The corresponding maximum internal image stress is $\sigma_{\text{int}} = 6.7 \text{ MPa}$, which is much smaller than the typical values of applied shear stresses (20–1000 MPa). For this particular case it appears that the image effects due to the periodic cell are quite small.

4. Motion of an initially straight edge dislocation

We apply a constant shear stress using the Parrinello–Rahman method [11] on the configuration of a straight edge dislocation prepared above. The shear stress σ_{xy} has components indicated in Fig. 1. A soft velocity scaler [12] is used to maintain the system at constant temperature.

During the simulation, the two dislocations are observed to move in opposite directions on their $(\bar{1}01)$ glide planes and after a short transient period, typically around 5 ps, achieve a steady-state motion with approximately constant speed. The instantaneous position of the dislocation core can be extracted on line from the maximum discrepancy between the two layer of atoms adjacent to the glide plane [13]. We find that essentially the same results are given by identifying core atoms through the measure of maximum local energies. A profile of the edge dislocation line as it glides at $T = 20 \text{ K}$ and $\sigma_{xy} = 50 \text{ MPa}$ is shown in Fig. 3. One can see that the dislocation moves by independent and spontaneous double-kink nucleation events, with essentially no spreading of a kink once it appears [13]. It can be inferred from Fig. 3 that the kink migration barrier is higher than that of kink nucleation, a behavior that can be confirmed by direct atomistic calculations involving only static relaxations [14].

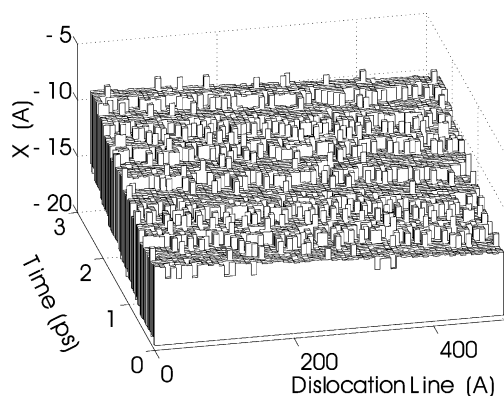


Fig. 3. Profile evolution of edge dislocation at motion by MD simulation under $T = 20$ K, $\sigma_{xy} = 50$ MPa. The dislocation seems to move by independent double-kink nucleation without appreciable contribution from kink migration.

5. Kink mobility on screw dislocation

Previous static atomistic simulations [15] suggest that a straight screw dislocation in Mo moves by double-kink mechanism, with a high double-kink nucleation barrier (~ 2 eV). At normal temperature (100–1000 K) and stress conditions (50–500 MPa), one therefore would not expect to be able to observe motion of a straight screw dislocation by MD. On the other hand, static atomistic simulations [16] also have found a very small migration barrier for kinks on screw dislocation, suggesting that a screw dislocation with a pre-existing density of kinks would be highly mobile. Taking the atomic simulation cell as shown in Fig. 2(b), we apply a shear stress $\sigma_{yz} = 100$ MPa at $T = 300$ K, and indeed we find that the screw dislocation starts moving via the translation of the kink along the dislocation line. The kink velocity is found to be $v = 600$ m/s, so that the phonon drag coefficient for the kink is $B \equiv \sigma \cdot b/v = 4.5 \times 10^{-5}$ Pa s. The drag coefficient for the edge dislocation at the same temperature is found to be $B = 1.8 \times 10^{-4}$ Pa s, which is about three times larger than that of the kink. This result is reasonable because a kink on the screw dislocation, being a short dislocation segment with an edge component, should move faster than a long edge dislocation.

6. Summary

We have demonstrated how motions of edge and screw dislocations induced by an applied shear stress can be directly observed by MD simulation of dislocation dipoles with PBC. In the case of an edge dislocation in bcc Mo described by an empirical interatomic potential, the effects of image interaction associated with PBC are found to be small. The profile of edge dislocation in motion obtained using an energy-based measure in tracking the dislocation core is generally consistent with our previous result based on locating maximum disorder between atom rows, both showing double-kink nucleation as the controlling mechanism for motion. Kink mobility on a screw dislocation appears to be about three times greater than that for a straight edge dislocation; however, this result is quite preliminary because the internal stress variation is found to be large in these simulations. We are using linear elasticity theory to design new simulation cell geometries in which the internal stress variation can be made negligible [6].

Acknowledgements

This work was supported by Lawrence Livermore National Laboratory under an ASCI-Level 2 project.

References

- [1] J.M. Rickman, S.R. Phillpot, D. Wolf, D.L. Woodraska, S. Yip, On the mechanism of grain-boundary migration in metals: a molecular dynamics study, *J. Mater. Res.* 6 (1991) 2291.
- [2] M.S. Duesbery, V. Vitek, *Acta Mater.* 46 (1998) 1481.
- [3] V.V. Bulatov, L.P. Kubin, *Curr. Opin. Solid State Mater. Sci.* 3 (1998) 558.
- [4] M.S. Daw, M.I. Baskes, C.L. Bisson, W.G. Wolfer, *Modeling Environmental Effects on Crack Growth Processes*, TMS-AIME, New York, 1986.
- [5] A. Moncevicz, P.C. Clapp, J.A. Rifkin, *Defects in Materials Symposium*, Boston, MA 1990, MRS; Pittsburgh, PA, 1990.
- [6] W. Cai, V.V. Bulatov, J. Chang, J. Li, S. Yip, *Phys. Rev. Lett.* 86 (2001) 5727.
- [7] M.W. Finnis, J.E. Sinclair, *Philos. Mag. A* 50 (1984) 45.

- [8] G.J. Ackland, R. Thetford, *Philos. Mag. A* 56 (1987) 15.
- [9] One can obtain displacement fields of an isolated dislocation from: J.P. Hirth, J. Lothe, *Theory of Dislocations*, Wiley, New York, 1982, Chapter 3, and then sum up the displacement fields of the primary and image dislocation dipoles.
- [10] More atoms are inserted to fill the empty lattice sites between the two cells. The positions of these lattice sites can be calculated from linear elasticity theory [9] Chapter 4.
- [11] M. Parrinello, A. Rahman, *Phys. Rev. Lett.* 45 (1980) 1196.
- [12] H. Andersen, *J. Chem. Phys.* 72 (1980) 2384.
- [13] J. Chang, W. Cai, V.V. Bulatov, S. Yip, *Mater. Sci. Eng. A* 309 (2001) 160.
- [14] V.V. Bulatov, S. Yip, A.S. Argon, *Philos. Mag. A* 72 (1995) 453.
- [15] W. Xu, J. Moriarty, *Dislocations Comput. Mater. Sci.* 9 (1998) 348.
- [16] J. Moriarty, M.S. Duesbery, private communication.